

Surface Waves in Oversized G-Band Slow-Wave Structures with Rectangular Corrugations^{*})

Kazuo OGURA, Akihiko KOJIMA, Fumiaki KAWABE, Kiyoyuki YAMBE and Md. Ruhul AMIN¹⁾

Graduate School of Science and Technology, Niigata University, Niigata 950-2181, Japan

¹⁾*Department of Electrical and Electronic Engineering, Islamic University of Technology, Gazipur 1704, Bangladesh*

(Received 6 December 2013 / Accepted 1 February 2014)

Surface waves in oversized G-band slow-wave structure with rectangularly corrugated wall are analyzed numerically. The inner corrugation generates cylindrical surface wave. The outer corrugation also generates transverse magnetic surface wave. The upper cut-offs of surface waves are controlled by corrugation amplitude. In excitation of the surface waves by an annular electron beam, the slow cyclotron interaction as well as the Cherenkov interaction occur due to there-dimensional beam perturbations. The slow cyclotron interaction merges with the Cherenkov interaction at lower magnetic field. The merged growth rate is enhanced by 13 % as compared to the isolated Cherenkov growth rate. The surface waves on inner and outer corrugations can have different frequencies and can be excited selectively by adjusting the beam radius of the electron beam.

© 2014 The Japan Society of Plasma Science and Nuclear Fusion Research

Keywords: oversized coaxial slow-wave structure, G-band, surface wave, Cherenkov interaction, slow cyclotron interaction, there-dimensional beam perturbation

DOI: 10.1585/pfr.9.3406022

1. Introduction

Smith-Purcell free electron lasers (SP-FELs) [1–3] and backward wave oscillators (BWOs) [4–6] have been studied extensively to obtain high frequency and high power electromagnetic (EM) waves. In SP-FELs, electron beams pass near the grating and excite some of the spatial harmonics of grating leading to SP radiations [1]. The original SP radiations are spontaneous and essentially weak. Recently, “super-radiance” due to stimulated SP radiation is demonstrated in hundreds of GHz range (over the 300–900 μm wavelength range) [2]. This SP-FEL uses a beam of scanning electron microscope (SEM) with around 30–35 kV voltage and attract attention to develop a compact THz wave source. For the super-radiance, the interaction between the beam and the surface wave on the grating surface is essential. The electron beam is desirable to cover the entire surface of flat grating. However, in the realistic SP-FELs, pencil like beams partially covered the grating surface and the power levels were in the μW range [2].

The SP-FELs described above are commonly based on a plain geometry. Another realistic geometry is a cylindrical one, which has been used for high-power BWOs. BWOs have slow-wave structures (SWSs) to form slow waves with the phase velocity close to the beam velocity. To increase the operation frequency and the power handling capability, SWSs are made oversized with the diameter D larger than the free-space wavelength λ of output EM wave, i.e., $D/\lambda \gg 1$. The slow waves in oversized SWS are

surface waves concentrated in the vicinity of the walls like SP-FELs. Recently, performance of the weakly relativistic oversized BWO has been improved by using uniformly distributed annular electron beam of current on the order of 100 A. The radiation powers are about 500 kW (K-band) and about 200 kW (Q-band) [6]. The values of D/λ are about 2.5 for K-band and about 4.2 for Q-band.

Unlike eventually unbounded SP-FEL, oversized BWO is a bounded system in which EM wave’s reflection forms waveguide modes. In oversized BWOs aiming at high frequency operation, many waveguide modes exist and the mode competition becomes a serious problem. To reduce this problem and to improve oversized BWO operation, a coaxial SWS may be used as an alternative to hollow SWS. In a plain geometry, parallel-plate SWSs are used. In a pioneering work of the Ledatron, parallel-plate SWS was called Fabry-Perot resonator [7]. Recently, surface waves and SP traveling wave tube operation of the parallel-plate SWS have been studied in a frequency range around 100 GHz (W-band) [8]. Since cylindrical BWOs are suitable for high-power operations, it is important to study the surface waves of coaxial SWS in such high frequency ranges in order to realize high-power and high-frequency EM wave sources.

In realistic devices, strength of magnetic field is not so strong that the transverse beam perturbations can be ignored. For example, a magnetic field less than 1.0 T is used to guide an annular electron beam in the weakly relativistic oversized BWOs [6] and a magnetic field around 0.4 T was necessary for a ribbon-like beam focusing of Ledatron and SP-FEL [7, 9]. The three-dimensional (3D)

author’s e-mail: teogura@eng.niigata-u.ac.jp

^{*}) This article is based on the presentation at the 23rd International Toki Conference (ITC23).

beam perturbations lead to the slow cyclotron interaction as well as the Cherenkov interaction [10–14]. The slow cyclotron interaction is caused by the anomalous Doppler effect and essentially different from the fast cyclotron interaction, which is due to the normal Doppler effect. The surface wave properties together with the 3D beam perturbations are still unclear and should be studied more definitely, especially in high-frequency ranges.

In this paper, we analyze surface waves in oversized G-band SWS with rectangularly corrugated wall. The surface waves in this frequency range play an important role in nuclear fusion science and for development of high-frequency BWOs. The value of D/λ is about 17, which is much larger than that of K-band or Q-band SWS. Since the surface waves are concentrated very close to the corrugations, their analysis becomes very difficult due to numerical divergences in calculation processes. By improving our calculation method, the dispersion characteristics of the G-band SWS are examined for hollow and coaxial configurations. The surface waves on inner and outer corrugations are excited by an infinitesimally thin annular beam. The slow cyclotron interaction as well as the Cherenkov interaction with the surface waves in oversized G-band SWS are analyzed by considering 3D beam perturbations.

2. Numerical Model

The cylindrical coordinate system (r, φ, z) is used in this study. A rectangularly corrugated coaxial SWS is driven by an annular electron beam as shown in Fig. 1. The corrugation parameters are amplitude h , width d and period z_0 . The corrugation wave number is defined as $k_0 = 2\pi/z_0$. Average radii of the outer and inner corrugations are R_{out} and R_{in} , respectively. A guiding magnetic field B_0 is applied in the z -direction and an infinitesimally thin annular electron beam of radius R_b propagates along B_0 . We consider a linear model assuming a temporal and spatial phase factor of perturbed quantities of $\exp[i(k_z z + m\varphi - \omega t)]$. Here, m is the azimuthal mode number, the k_z is the axial wave number and ω is the angular frequency. In this paper, we analyze axially symmetric modes with $m = 0$.

In corrugation regions of $R_{\text{in}} - h < r < R_{\text{in}} + h$ and $R_{\text{out}} - h < r < R_{\text{out}} + h$, EM fields are expressed as a sum

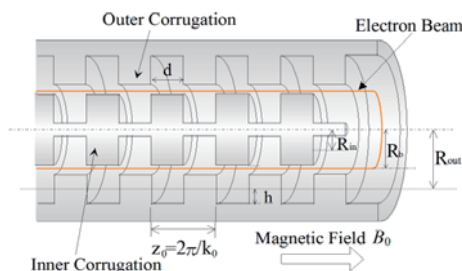


Fig. 1 Coaxial SWS driven by an infinitesimally thin annular electron beam.

of standing waves that satisfy the boundary conditions on the corrugation walls. In SWS waveguide regions of $R_{\text{in}} + h < r < R_b$ and $R_b < r < R_{\text{out}} - h$, EM fields are expanded in a spatial harmonic series in accordance with Floquet's theorem. EM fields in each region are correlated by using corresponding boundary conditions. The beam boundary correlates the Floquet's harmonics in the inner and outer regions of beam. The infinitesimally thin annular beam is modulated due to transverse perturbations. This modulated boundary is formulated in accordance with the method of Refs.13 and 14.

The eigen functions for cylindrical systems are the Bessel functions, i.e., J_m and N_m . They can be used for non-oversized SWSs in which EM modes are volumetric waves having the strong field near the axis. However, the surface waves in oversized SWS are localized very close to the SWS wall. If the Floquet's harmonics are expressed by J_m and N_m , they become extremely large leading to serious problems in numerical calculations. To avoid this problem, the modified Bessel functions, i.e., I_m and K_m are used instead of J_m and N_m . By improving our numerical method, the dispersion characteristics of the G-band SWS are examined for hollow and coaxial configurations.

3. Numerical Results

There are two cylindrical waveguide modes: transverse electric (TE) and transverse magnetic (TM) modes. The BWO operations are based on TM components. Figure 2 shows the axisymmetric TM modes in a hollow oversized SWS with $R_{\text{out}} = 15.0$ mm, in which the inner conductor is removed from Fig. 1. The corrugation has dimensions: $h = 0.15$ mm, $d = 0.30$ mm, $z_0 = 0.50$ mm and $k_0 = 125.6$ cm⁻¹. According to Floquet's theorem, the dispersion curves are periodic in the k_z -space with period k_0 . And TM modes lead to the slow-wave interactions. The lowest TM mode is TM_{01} and has an upper cut-off frequency of 168 GHz (G-band). Above TM_{01} mode, higher order modes starting from TM_{02} mode exit very closely to each other in the fast-wave regions. As a reference, the Cherenkov ($\omega = k_z v_0$) and slow cyclotron ($\omega = k_z v_0 - \Omega$)

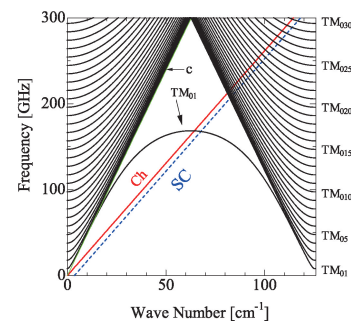


Fig. 2 Dispersion curves of hollow SWS with $R_{\text{out}} = 15.0$ mm. CH and SC are Cherenkov and slow cyclotron lines, respectively.

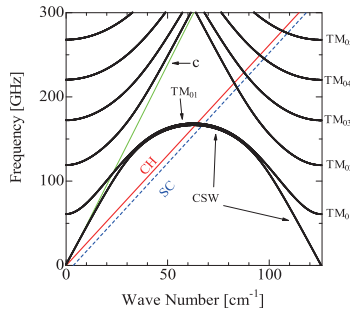


Fig. 3 Dispersion curves of coaxial SWS with $R_{out} = 15.0$ mm and $R_{in} = 12.6$ mm. Inner and outer corrugations have the same parameters. CH and SC are the same as Fig. 2.

lines are plotted with the beam energy of 100 keV and $B_0 = 0.4$ T.

Figure 3 shows the axisymmetric TM dominant modes in oversized coaxial SWS. The average radii are $R_{out} = 15.0$ mm (the same as Fig. 2) and $R_{in} = 12.6$ mm. The corrugation has the same G-band dimensions as Fig. 2. The inner conductor of coaxial SWS drastically reduces the higher order modes. Moreover, the inner conductor generates the fundamental transverse electromagnetic (TEM) mode. When the inner conductor is corrugated as shown in Fig. 1, the TEM mode becomes a TM dominant surface wave of the inner corrugation and is referred to as the cylindrical surface wave (CSW) [14]. CSW in Fig. 3 has an upper cut-off frequency of 166 GHz (G-band) and can exist even if the outer conductor is removed. The TM_{01} mode is the lowest waveguide mode of the outer corrugation with the same upper cut-off frequency of 168 GHz as that of Fig. 2.

The outer corrugation is formed on the concave side of the cylindrical surface. On the other hand, the inner corrugation is formed on the convex side of the cylindrical surface. The curvature effect of the convex curvature is opposite to that of the concave curvature [14]. And then the upper cut-off frequency is about 168 GHz for the TM_{01} surface wave and is slightly higher than 166 GHz for the CSW with the same h , d and z_0 . The upper cut-off of TM_{01} and CSW surface waves is controlled by h . In Fig. 4, the TM_{01} upper cut-off is decreased to about 150 GHz by increasing the outer h and the CSW upper cut-off is increased to about 175 GHz by decreasing the inner h . TM_{01} and CSW are crossing each other.

With an electron beam, the transverse beam perturbations in a finite B_0 combine the TM and the TE modes. And hence, EM waves become hybrid modes even in axisymmetric cases. The letters EH and HE are often used to designate the hybrid modes. This paper follows the definition in Ref. 12: the TM (TE) mode is dominant in the EH (HE) mode around $k_z = 0$. TM_{0s} modes without a beam in Figs. 2, 3 and 4 become EH_{0s} modes. Here, $s (= 1, 2, 3, \dots)$ is the mode number. Figure 5 shows temporal growth rates for coaxial SWS of Fig. 4 driven by an annular electron

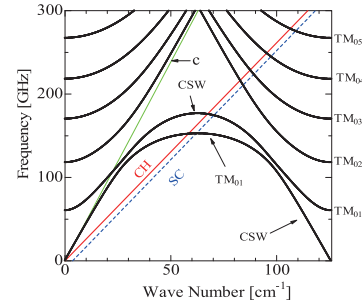


Fig. 4 Dispersion curves of coaxial SWS with the same parameters as Fig. 3, except for h . Outer h increases to 0.175 mm and inner h decreases to 0.135 mm. CH and SC are the same as Fig. 2.

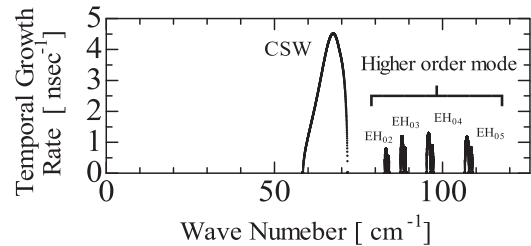


Fig. 5 Temporal growth rates in coaxial SWS with the same parameters as Fig. 4. An infinitesimally thin annular electron beam has $R_b = 12.8$ mm. And $B_0 = 0.4$ T.

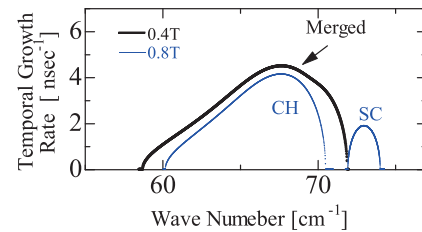


Fig. 6 Temporal growth rates in coaxial SWS with the same corrugation and beam as in Fig. 5 with $B_0 = 0.4$ T and 0.8 T.

beam with energy of 100 keV, current of 200 A and $R_b = 12.8$ mm. The beam propagates close to the inner corrugations and interacts with only CSW. In Fig. 5, CSW growth rate is a merged one of the Cherenkov and slow cyclotron growth rates, which is called “merged growth rate” [12]. The Cherenkov and slow cyclotron growth rates exist separately with a sufficiently strong B_0 and merge around $B_0 = 0.4$ T as shown in Fig. 6. The merged growth rate increases by 13 % from the isolated Cherenkov growth rate with $B_0 = 0.8$ T.

Excitations of CSW and EH_{01} surface waves strongly depend on the beam radius as shown in Fig. 7. The merged growth rate of CSW with $R_b = 12.8$ mm splits into the Cherenkov and slow cyclotron growth rates with $R_b > 13.0$ mm. The growth rates for CSW decrease by increasing with R_b and become negligible beyond $R_b = 13.8$ mm, the center of inner and outer corrugations. In

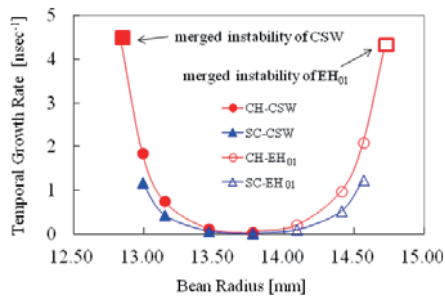


Fig. 7 Peak temporal growth rates versus beam radius.

the region of $R_b > 13.8$ mm, the growth rates for EH_{01} become dominant and increase by increasing R_b . With $R_b = 14.7$ mm, the merged growth rate is formed again and is nearly the same as that of CSW with $R_b = 12.8$ mm. The frequencies of excited CSW and the EH_{01} are controlled by h as can be seen in Fig. 4. And the CSW and the EH_{01} with the different frequencies can be excited selectively by adjusting the beam's radius. Near the corrugations, the Cherenkov and slow cyclotron interactions become so strong that they form a merged growth.

4. Discussion and Conclusion

There are two mechanisms of the Cherenkov interaction. One is the conventional mechanism attributed to a longitudinal perturbation. The other is attributed the transverse perturbation of the beam surface [15]. The coupling via the longitudinal beam perturbation is weakened by decreasing B_0 as pointed out in Ref. 8. On the other hand, the transverse beam perturbation, i.e., the modulation of beam surface dominates the Cherenkov interaction in the low magnetic field region [15]. The transverse perturbation also causes the slow cyclotron interaction with the same order strength as the Cherenkov interaction as shown in Fig. 6. And the merged growth is formed for low value of B_0 . This is in contrast to non-oversized case, where the slow cyclotron interaction has one order smaller growth rate than the Cherenkov one and is suppressed by the Cherenkov interaction in the low magnetic field region [16].

In conclusion, surface waves in oversized G-band SWS with rectangularly corrugated wall are analyzed numerically. The value of D/λ is about 17, which is much

greater than those of K-band and Q-band SWS. By developing numerical codes, the dispersion characteristics of the G-band SWS are examined for hollow and coaxial configurations. The outer and inner

corrugations generate surface waves with upper cut-offs in the G-band. The upper cut-offs of surface waves are controlled by corrugation amplitude. The slow cyclotron interaction as well as the Cherenkov interaction occur due to 3D beam perturbations. Two interactions form a merged growth for low value of B_0 . The merged growth rate is enhanced by 13% as compared to the isolated Cherenkov growth rate. Excitations of surface waves strongly depend on the beam radius. The surface waves on the inner and corrugations can have different frequencies and can be excited selectively by adjusting the beam's radius. The controllability of surface wave and their excitation may be of considerable interest for developing tunable high-frequency BWOs.

Acknowledgments

This work was partially supported by Grant-in-Aid for Scientific Research (B) No. 23340173 from the Japan Society for the Promotion of Science and by the NIFS collaboration research program No. NIFS12KLER014.

- [1] S.J. Smith and E.M. Purcell, Phys. Rev. **92**, 1069 (1953).
- [2] J. Urata *et al.*, Phys. Rev. Lett. **80**, 516 (1998).
- [3] H.L. Andrews *et al.*, Phys. Rev. ST Accel. Beams **12**, 080703 (2009).
- [4] A.V. Gunin *et al.*, IEEE Trans. Plasma Sci. **26**, 326 (1998).
- [5] A.N. Vlasov *et al.*, IEEE Trans. Plasma Sci. **28**, 550 (2000).
- [6] S. Aoyama *et al.*, Trans. Fusion Sci. Tech. **51**, 325 (2007).
- [7] K. Mizuno *et al.*, IEEE Trans. Electron Devices **20**, 749 (1973).
- [8] H.P. Freund *et al.*, IEEE Trans. Plasma Sci. **32**, 1015 (2004).
- [9] V. Kumer *et al.*, Phys. Rev. ST Accel. Beams **12**, 070703 (2009).
- [10] Md. R. Amin *et al.*, J. Phys. Soc. Jpn. **64**, 4473 (1995).
- [11] K. Ogura *et al.*, Phys. Rev. E **53**, 2726 (1996).
- [12] O. Watanabe *et al.*, Phys. Rev. E **63**, 056503 (2001).
- [13] K. Ogura *et al.*, J. Plasma Phys. **72**, 905 (2006).
- [14] K. Ogura *et al.*, IEEE Trans. Plasma Sci. **41**, 2729 (2013).
- [15] K. Ogura *et al.*, J. Phys. Soc. Jpn. **67**, 3462 (1998).
- [16] H. Yamazaki *et al.*, IEEJ Trans. FM **124**, 477 (2004).